AMERICAN SCIENTIFIC PUBLISHERS

Reviews in Theoretical Science
Vol. 4, pp. 1–14, 2016
(www.aspbs.com/rits)

Multiband Superconductors

S. P. Kruchinin

Bogolyubov Institute for Theoretical Physics, Ukrainian National Academy of Science, Kiev 03680, Ukraine

In this review concentrates on the multiband superconductivity. We consider the physical properties of superconductor MgB_2 and use our two-band model to explain the two coupled superconductor's gaps of MgB_2. To study the effect of the increasing T_c in MgB_2, we used the renormalization group approach and phase diagrams. In the field of superconductivity we Meet the problem-maximum which consists in the creation of room-temperature superconductors. We consider this problem in our review and make some recommendations on the search for these superconductors.

KEYWORDS: Multiband, Superconductors, Room Temperature Superconductor, Phase Diagram, Two-Gap Superconductivity, Two-Band, MgB_2.

CONTENTS

1. Introduction 1
2. Multiband Hamiltonian 2
2.1. Hamiltonian 2
2.2. Two-Particle Green Function 3
2.3. Traditional Superconductivity 4
2.4. Copper Oxides 4
2.5. Cooperative Mechanism 5
2.6. Room-Temperature Superconductors 5
3. Two-Gap Superconductivity in MgB_2 6
3.1. The Physical Properties of MgB_2 6
3.2. Theoretical Model 7
3.3. Superconductivity in MgB_2 8
4. Theoretical Studies of Multiband Effects in Superconductivity by Using The Renormalization Group Approach 10
4.1. Theoretical Model 10
4.2. Renormalization-Group Approach 11
4.3. Vertex Correction and Response Function for Cooper Pairs 11
4.4. Renormalization Equation 12
4.5. Phase Diagrams 12
5. Summary 13
References and Notes 13

1. INTRODUCTION

In this chapter, we present the theory of superconductivity with regard to a complicated multiband structure of superconductors. Calculations of the band structure of cuprate superconductors indicate that several energy bands intersect one another on the Fermi surface in these compounds,[1] and the Fermi surface passes through high-symmetry points which correspond to the Lifshitz electronic topological transition. In addition, the discovery of two-gap superconductivity in two-band superconductors MgB_2 allows one to consider the possibility of using a multiband theory of superconductivity. In Section 2, we analyze the problems of multiband superconductivity and superconductivity at room temperature. In Section 3, we study the physical properties of superconductors MgB_2 and problems of two-gap superconductivity, as well as the phase diagram for superconductors MgB_2 on the basis of the renormalization group approach. In the field of superconductivity, we meet the problem-maximum—the creation of room-temperature superconductors. We consider this problem in our book and give some recommendations on the search for these superconductors. The discovery of new class of high-temperature superconductors—Fe based layered compounds—aroused a significant interest at the beginning of 2008 and gave hope for a progress in the synthesis of novel high-Tc superconductors up to room-temperature superconductors. This superconductors belong to multiband superconductivity , involving from 2 to 5 bands.[9] The results of this review were obtained by the authors and published in Refs. [1–8].

The theory of superconductivity arising from the electron-phonon interaction mechanism by Bardeen, Cooper and Schrieffer (BCS)[9] has been well established, and it is now the standard theory for superconductivity.[9–14] In review,[10] we have considered non-BCS mechanisms via spin fluctuations, charge fluctuations (plasmons) and electron excitations (excitons), which have attracted great interest, for example in relation to the possibility of high-T_c superconductivity. These mechanisms have the common characteristic that the electron–electron (e–e) interaction is an origin of the superconductivity. After the discovery of the high-T_c copper oxides,[13] Anderson[14] emphasized an important role of the e–e interaction. Over the past decade, many non-BCS theories[15–20] have been proposed, but they do not converge as a unified and

Email: sergeikruchinin@yahoo.com
Received: 3 February 2015
Accepted: 24 February 2015

well-accepted theory yet. On the other hand, experimental studies on copper oxides have revealed the following characteristics:
(1) These species are antiferromagnets before doping, in accordance with the importance of the e–e interaction;
(2) The high-T_c superconductivity appears in the intermediate region of the metal-insulator transition and disappears in the metallic or overdoped region.[21–23]

Accumulated experimental results on the species and related materials suggest a guiding principle that the doping in magnetic systems, more generally charge-transfer (CT) insulators, may provide several exotic phases which are
(a) Ferromagnetic metal or insulator,
(b) Spin glass,
(c) Paramagnetic metals,
(d) Antiferromagnetic metals,
(e) Ferrimagnetic metal or insulator,
(f) Charge- or spin-mediated superconductor.

Relative stabilities of these phases should be dependent on several factors. The theoretical description of such phases and phase transitions in a systematic fashion is quite hard. Recently, the importance of multiband effects in high-T_c superconductivity has been pointed out.[8, 9, 11] In the framework of the two-particle Green function techniques,[3, 6] it is shown that a class of new so-called coupled states arises in the electron-phonon system. The model numerical calculations have shown that the superconducting (SC) gap depends on the number of bands crossing the Fermi level, and the temperature dependence of the SC gap for high-T_c superconductors is more complicated than that predicted in the BCS approach. We have also investigated anomalous phases in a two-band model by using the Green function techniques.[24, 25] The expressions for the transition temperature for several phases have been derived, and the approach has been applied to the superconductivity in molecular crystals by charge injection and field-induced superconductivity.

In this review, we investigate the superconductivity by using the two-band model and the two-particle Green function technique. In the framework of the two-band model, the coupled states in the electron system and the conditions under which the coupled states can appear are investigated. We apply the model to the electron-phonon mechanism within the traditional BSC method, the electron–electron interaction mechanism for high-T_c superconductivity, and the cooperative mechanism in relation to the multiband superconductivity.

2. MULTIBAND HAMILTONIAN

In this section, we summarize the two-band model for superconductivity, introduce a two-particle Green function and investigate the spectral properties of the model.

2.1. Hamiltonian

We start from the Hamiltonian for two bands i and j:

$$H = H_0 + H_{\text{int}} \tag{1}$$

with

$$H_0 = \sum_{\mathbf{k},\sigma} [[\varepsilon_i - \mu] a^+_{i\mathbf{k}\sigma} a_{i\mathbf{k}\sigma} + [\varepsilon_j - \mu] a^+_{j\mathbf{k}\sigma} a_{j\mathbf{k}\sigma}] \tag{2}$$

$$\begin{aligned} H_{\text{int}} = \frac{1}{4} \sum_{\delta(\mathbf{p}_1+\mathbf{p}_2,\,\mathbf{p}_3+\mathbf{p}_4)} \sum_{\alpha\beta\gamma\delta} [&\Gamma^{iiii}_{\alpha\beta\gamma\delta} a^+_{i\mathbf{p}_1\alpha} a^+_{i\mathbf{p}_2\beta} a_{i\mathbf{p}_3\gamma} a_{i\mathbf{p}_4\delta} \\ &+ (i \to j) + \Gamma^{iijj}_{\alpha\beta\gamma\delta} a^+_{i\mathbf{p}_1\alpha} a^+_{i\mathbf{p}_2\beta} a_{j\mathbf{p}_3\gamma} a_{j\mathbf{p}_4\delta} + (i \to j) \\ &+ \Gamma^{ijij}_{\alpha\beta\gamma\delta} a^+_{i\mathbf{p}_1\alpha} a^+_{j\mathbf{p}_2\beta} a_{i\mathbf{p}_3\gamma} a_{j\mathbf{p}_4\delta} + (i \to j)] \end{aligned} \tag{3}$$

Sergei Kruchinin (1957)—is leading scientist of the Bogolyubov Institute for Theoretical Physics, NASU (Kiev, Ukraine). Professor of at the National Aviation University. S. P. Kruchinin has published significant original works in the fields of nuclear physics and many-particle systems, solid-state physics, superconductivity, theory of nonlinear phenomena, nanophysics. He is the author and co-author of more than 100 scientific works which have been published in leading scientific journals. He has been using advanced mathematical methods to solve the posed problems. Since the time high-temperature superconductors were discovered, S. P. Kruchinin has intensively studied their physical properties. In particular, it is worth noting the work carried out jointly with A. S. Davydov "Interlayer Effects in the Newest High-Tc Superconductors" (Physica C, 1991), where the theory of the non-monotonous dependence of the critical temperature of superconductivity on the number of cuprate layers in the elementary cell of high-temperature superconductors was developed. This work has remained up to date in connection with the search for new superconductors operating at room temperature. Kruchinin's works on superconductivity were included in the monograph "Modern aspects of Superconductivity: Theory of Superconductivity" (World Scientific, Singapore, 2010, jointly with H. Nagao) which shows the contemporary status of the problems of high-temperature superconductivity. He has published the textbook "Theory of Field. Solution of the problems" for students. Kruchinin was the organizer of seven international conferences on the current problems of high-temperature superconductivity and nanosystems. Six books in Springer and one book in World Scientific publishing houses were published under his guidance. Kruchinin Sergei is the co-editor of the following journals: "Quantum Matter" (USA), "Reviews in Theoretical Science" (USA), "Progress in Nanotechnology and Nanomaterials" (USA).

where Γ is the bare vertex part,

$$\Gamma^{ijkl}_{\alpha\beta\gamma\delta} = \langle i\mathbf{p}_1\alpha j\mathbf{p}_2\beta|k\mathbf{p}_3\gamma l\mathbf{p}_4\delta\rangle\delta_{\alpha\delta}\delta_{\beta\gamma} - \langle i\mathbf{p}_1\alpha j\mathbf{p}_2\beta|l\mathbf{p}_4\delta k\mathbf{p}_3\gamma\rangle\delta_{\alpha\gamma}\delta_{\beta\delta} \quad (4)$$

with

$$\langle i\mathbf{p}_1\alpha j\mathbf{p}_2\beta|k\mathbf{p}_3\gamma l\mathbf{p}_4\delta\rangle = \int d\mathbf{r}_1 d\mathbf{r}_2 \phi^*_{i\mathbf{p}_1\alpha}(\mathbf{r}_1)\phi^*_{j\mathbf{p}_2\beta}(\mathbf{r}_2) \times V(\mathbf{r}_1,\mathbf{r}_2)\phi_{k\mathbf{p}_3\gamma}(\mathbf{r}_2)\phi_{l\mathbf{p}_4\delta}(\mathbf{r}_1) \quad (5)$$

and $a^+_{ip\sigma}$ ($a_{ip\sigma}$) is the creation (annihilation) operator corresponding to the excitation of electrons (or holes) in the ith band with spin σ and momentum $\mathbf{p}$, μ is the chemical potential and $\phi^*_{ip\alpha}$ is a single-particle wave function. Here, we suppose that the vertex function in Eq. (3) consists of the effective interactions between the carriers caused by the linear vibronic coupling in several bands and the screened Coulombic interband interaction of carriers. When we use the two-band Hamiltonian (1) and define the order parameters for the singlet exciton, triplet exciton and singlet Cooper pair, the mean field Hamiltonian is easily derived.[1–5, 25, 26] Here, we focus on four-electron scattering processes:

$$g_1 = \langle ii \mid ii\rangle = \langle jj \mid jj\rangle \quad (6)$$

$$g_2 = \langle ii \mid jj\rangle = \langle jj \mid ii\rangle \quad (7)$$

$$g_3 = \langle ij \mid ij\rangle = \langle ji \mid ji\rangle \quad (8)$$

$$g_4 = \langle ij \mid ji\rangle = \langle ji \mid ij\rangle \quad (9)$$

g_1 and g_2 represent the intraband two-particle normal and umklapp scatterings respectively, g_3 is the interband two-particle umklapp process and g_4 indicates the interband two-particle interaction on different bands (see Fig. 1). Note that Γ's are given by

$$\Gamma^{iiii}_{\alpha\beta\gamma\delta} = \Gamma^{jjjj}_{\alpha\beta\gamma\delta} = g_1(\delta_{\alpha\delta}\delta_{\beta\gamma} - \delta_{\alpha\gamma}\delta_{\beta\delta})$$
$$\Gamma^{iijj}_{\alpha\beta\gamma\delta} = \Gamma^{jjii}_{\alpha\beta\gamma\delta} = g_2(\delta_{\alpha\delta}\delta_{\beta\gamma} - \delta_{\alpha\gamma}\delta_{\beta\delta})$$
$$\Gamma^{ijij}_{\alpha\beta\gamma\delta} = \Gamma^{jiji}_{\alpha\beta\gamma\delta} = g_3\delta_{\alpha\delta}\delta_{\beta\gamma} - g_4\delta_{\alpha\gamma}\delta_{\beta\delta} \quad (10)$$

where an antisymmetrized vertex function Γ is considered to be a constant independent of the momenta.

The spectrum is elucidated by the Green function method. Using Green functions which characterize the CDW (charge-density-wave), SDW (spin-density-wave) and SSC (singlet superconducting) phases, we obtain a self-consistent equation, according to the traditional procedure.[1, 24–26] Then, we can obtain expressions for the transition temperature for some cases.

In the framework of the one-band model, the electronic phases are characterized by

$$-g_2 - 2g_3 + g_4 > 0 \quad \text{for CDW}$$
$$g_2 + g_4 > 0 \quad \text{for SDW}$$
$$-g_1 > 0 \quad \text{for SSC}$$

In the framework of the two-band model, we have already derived expressions of the transition temperature for CDW, SDW and SSC. In the previous papers,[1, 24–26] we have investigated the dependence of T_c on the hole or electron concentration for the superconductivity of copper oxides by using the two-band model and have obtained a phase diagram of $Bi_2Sr_2Ca_{1-x}Y_xCu_2O_8$ (Bi-2212) by means of the above expressions for the transition temperature. The dependence of T_c on Δp can be reproduced in agreement with the experiment.[1, 24–26] Recently, we have also obtained phase diagrams of copper oxides, anthracene, oligothiophene and C_{60} crystals by using the analytic solutions.[1, 24–26]

2.2. Two-Particle Green Function

In this subsection, we introduce a two-particle Green function[1–3] to investigate the physical properties of superconductivity in the two-band model. In statistical mechanics, Green functions are a convenient generalization of the notion of correlation functions. Like the latter, the former are closely related to the calculations of observables and give the well-known advantages in the construction and the solution of equations. First, let us define one-particle Green functions:

$$G^{\nu}_{\sigma}(\mathbf{k}, t'-t) = \langle -iT[a_{\nu\mathbf{k}\sigma}(t)a^+_{\nu\mathbf{k}\sigma}(t')]\rangle \quad (11)$$

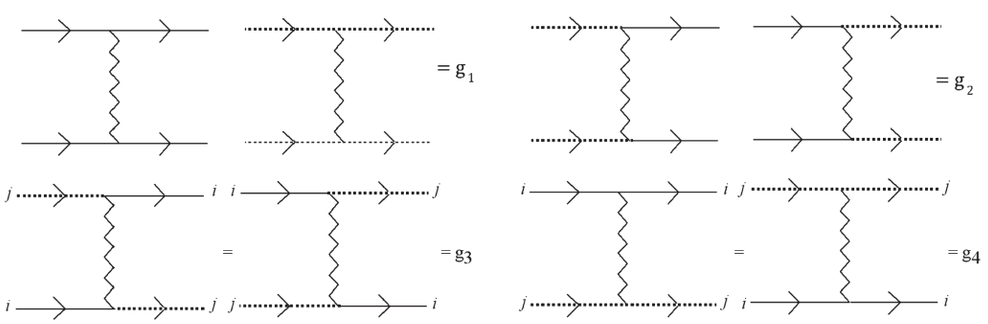

Fig. 1. Electron–electron interactions. Dependence of g on the direction in the momentum space is ignored in this model [$g_x(\mathbf{k}) \approx g_x$ $(x = i, j)$]. We assume that g_x is constant.

where σ and ν represent labels for a spin and a band, respectively. The equation for a Green function derived by using the two-band model (1) is written as

$$i\frac{\partial}{\partial t}\langle -iT[a_{\nu\mathbf{k}\sigma}(t)a^{+}_{\nu\mathbf{k}\sigma}(t')]\rangle = \delta(t-t')+\left\langle -iT\left[i\frac{\partial a_{\nu\mathbf{k}\sigma}(t)}{\partial t}a^{+}_{\nu\mathbf{k}\sigma}(t')\right]\right\rangle \quad (12)$$

where

$$i\frac{\partial a_{\nu\mathbf{k}\sigma}(t)}{\partial t} = [a_{\nu\mathbf{k}\sigma}, H] \quad (13)$$

The equation for the Green function (12) is rewritten after inserting Eq. (13) as

$$\begin{aligned} i\frac{\partial}{\partial t}&\langle -iT[a_{\nu\mathbf{k}\sigma}(t)a^{+}_{\nu\mathbf{k}\sigma}(t')]\rangle \\ &= \delta(t-t')+[\varepsilon_\nu-\mu]\langle -iT[a_{\nu\mathbf{k}\sigma}(t)a^{+}_{\nu\mathbf{k}\sigma}(t')]\rangle \\ &\quad+\frac{1}{2}\sum_{\beta\gamma\delta}\sum_{\delta(\mathbf{k}+\mathbf{p}_2,\,\mathbf{p}_3+\mathbf{p}_4)} g_1(\delta_{\sigma\delta}\delta_{\beta\gamma}-\delta_{\sigma\gamma}\delta_{\beta\delta}) \\ &\quad\times G^{\gamma\delta\beta\sigma}_{2_{\nu\nu\nu\nu}}(\mathbf{p}_3,\mathbf{p}_4,\mathbf{p}_2,\mathbf{k};t,t') \\ &\quad+\frac{1}{2}\sum_{\nu'}\sum_{\beta\gamma\delta}\sum_{\delta(\mathbf{k}+\mathbf{p}_2,\mathbf{p}_3+\mathbf{p}_4)} g_2(\delta_{\sigma\delta}\delta_{\beta\gamma}-\delta_{\sigma\gamma}\delta_{\beta\delta}) \\ &\quad\times G^{\gamma\delta\beta\sigma}_{2_{\nu'\nu'\nu\nu}}(\mathbf{p}_3,\mathbf{p}_4,\mathbf{p}_2,\mathbf{k};t,t') \\ &\quad+\frac{1}{2}\sum_{\nu'}\sum_{\beta\gamma\delta}\sum_{\delta(\mathbf{k}+\mathbf{p}_2,\mathbf{p}_3+\mathbf{p}_4)} (g_3\delta_{\sigma\delta}\delta_{\beta\gamma}-g_4\delta_{\sigma\gamma}\delta_{\beta\delta}) \\ &\quad\times G^{\gamma\delta\beta\sigma}_{2_{\nu\nu'\nu'\nu}}(\mathbf{p}_3,\mathbf{p}_4,\mathbf{p}_2,\mathbf{k};t,t') \end{aligned} \quad (14)$$

where

$$G^{\gamma\delta\beta\sigma}_{2_{\nu\nu\nu\nu}}(\mathbf{p}_3,\mathbf{p}_4,\mathbf{p}_2,\mathbf{k};t,t') = \langle -iT[a_{\nu\mathbf{p}_3\gamma}(t)a_{\nu\mathbf{p}_4\delta}(t)a^{+}_{\nu\mathbf{p}_2\beta}(t-0)a^{+}_{\nu\mathbf{k}\sigma}(t')]\rangle \quad (15)$$

$$G^{\gamma\delta\beta\sigma}_{2_{\nu'\nu'\nu\nu}}(\mathbf{p}_3,\mathbf{p}_4,\mathbf{p}_2,\mathbf{k};t,t') = \langle -iT[a_{\nu'\mathbf{p}_3\gamma}(t)a_{\nu'\mathbf{p}_4\delta}(t)a^{+}_{\nu\mathbf{p}_2\beta}(t-0)a^{+}_{\nu\mathbf{k}\sigma}(t')]\rangle \quad (16)$$

$$G^{\gamma\delta\beta\sigma}_{2_{\nu\nu'\nu'\nu}}(\mathbf{p}_3,\mathbf{p}_4,\mathbf{p}_2,\mathbf{k};t,t') = \langle -iT[a_{\nu\mathbf{p}_3\gamma}(t)a_{\nu'\mathbf{p}_4\delta}(t)a^{+}_{\nu'\mathbf{p}_2\beta}(t-0)a^{+}_{\nu\mathbf{k}\sigma}(t')]\rangle \quad (17)$$

ν' indicates a band different from ν. To calculate the density of electron states, we have to focus on the case where $t'\to t-0$. The two-particle Green functions in Eq. (14) is rewritten as $G_2(\mathbf{p}_3,\mathbf{p}_4,\mathbf{p}_2,\mathbf{k};t-t')(t'\to t-0)$.

In this study, we investigate only the spectral properties of two-particle Green functions for the superconductivity. Therefore, we focus on the following two-particle Green function:

$$G^{\gamma\delta\beta\sigma}_{2_{\nu\nu\nu\nu}}(\mathbf{p}_3,\mathbf{p}_4,\mathbf{p}_2,\mathbf{k};t,t') = \langle -iT[a_{\nu\mathbf{p}_3\gamma}(t)a_{\nu\mathbf{p}_4\delta}(t)a^{+}_{\nu\mathbf{p}_2\beta}(t')a^{+}_{\nu\mathbf{k}\sigma}(t')]\rangle \quad (18)$$

For simplicity, we consider only three cases:
(i) $g_1\neq 0$ and others = 0
(ii) $g_2\neq 0$ and others = 0
(iii) $g_1\neq 0$, $g_2\neq 0$ and others = 0.

2.3. Traditional Superconductivity

In general, in the framework of the BCS theory, the Hamiltonian is described by a single-band model. In the effective electron–electron interaction (Eq. (1)), we consider that $g_1\neq 0$ and others = 0 and focus only on the single-band model. According to the approach 101 used for phonon systems which is based on the method of Bogoliubov and Tyablikov,[27] we can derive the equation for a two-particle electron Green function. The spectral features of the electron system in the mentioned region of energy are described by the Fourier transform of this function. For the simplest case of a one-electron zone crossing the Fermi energy level, it can be given as

$$G^{\gamma\delta\beta\sigma}_{2_{\nu\nu\nu\nu}}(\mathbf{p}_3,\mathbf{p}_4,\mathbf{p}_2,\mathbf{k};t-t') = \frac{f(\mathbf{k},\mathbf{k}',\omega)\sum_{\sigma,\sigma'}\phi(\sigma,\sigma')}{1-g_1\sum_{\mathbf{q}}K(\omega,\mathbf{k},\mathbf{k}',\mathbf{q})} \quad (19)$$

where

$$K(\omega,\mathbf{k},\mathbf{k}',\mathbf{q}) = \frac{2-n^{\nu}_{\mathbf{k}+\mathbf{q}}-n^{\nu}_{\mathbf{k}'-\mathbf{q}}}{2\omega-\varepsilon^{\nu}_{\mathbf{k}+\mathbf{q}}-\varepsilon^{\nu}_{\mathbf{k}'-\mathbf{q}}} \quad (20)$$

n_k indicates the filling number of electrons and g_1 is the effective Fourier transform of the e–e interaction. If the e–e interaction constant renormalized by the electron-phonon interaction becomes negative, coupled states will appear in the electron system. In the previous papers,[1–3] we have presented analysis of the spectral properties of the two-particle Green function. According to the same procedure,[1–3] we obtain the equation for coupled states in the electron system:

$$1-g_1N(\varepsilon_f)\left[-\ln\left|1-\frac{\Delta}{a}\right|\right]=0 \quad (21)$$

where

$$N(\varepsilon_f) = \sqrt{2}\pi m^*_\nu\sqrt{m^*_\nu\varepsilon}(2-n^{\nu}_{\mathbf{k}+\mathbf{q}}-n^{\nu}_{\mathbf{k}'-\mathbf{q}})|_{\varepsilon=\varepsilon_f} \quad (22)$$

$$n^{\nu}_{\mathbf{k}} = \frac{1}{\exp[(\varepsilon^{\nu}_{\mathbf{k}}-\varepsilon_f)/T]+1} \quad (23)$$

$a=2(\omega-\varepsilon_f-\Delta_\nu-E)$, $E=k^2/2m$, $\varepsilon=q^2/2m$ and $m^*_\nu=m_\nu/m$. m^*_ν means the reduced effective mass of the electron in the crystal energy zone. m is the mass of the free electron. If $g_1<0$, we can find solutions to Eq. (21) for superconductivity.

2.4. Copper Oxides

In copper oxides, the effective e–e interaction g_2 is important for realizing the high-T_c superconductivity.[28,29] Therefore, we consider that $g_2\neq 0$ and others $=0$. The two-particle Green function (18) is rewritten as

$$G^{\gamma\delta\beta\sigma}_{2_{\nu\nu\nu\nu}}(\mathbf{p}_3,\mathbf{p}_4,\mathbf{p}_2,\mathbf{k};t-t') = \frac{f(\mathbf{k},\mathbf{k}',\omega)\sum_{\sigma,\sigma'}\phi(\sigma,\sigma')}{1-g_2^2\sum_{\mathbf{q},\mathbf{q}'}K_2(\omega,\mathbf{k},\mathbf{k}',\mathbf{q},\mathbf{q}')} \quad (24)$$

where

$$K_2(\omega, \mathbf{k}, \mathbf{k}', \mathbf{q}, \mathbf{q}') = \frac{(2 - n^{\nu'}_{\mathbf{k}+\mathbf{q}-\mathbf{q}'} - n^{\nu'}_{\mathbf{k}'-\mathbf{q}+\mathbf{q}'})(2 - n^{\nu}_{\mathbf{k}+\mathbf{q}} - n^{\nu}_{\mathbf{k}'-\mathbf{q}})}{(2\omega - \varepsilon^{\nu'}_{\mathbf{k}+\mathbf{q}-\mathbf{q}'} - \varepsilon^{\nu'}_{\mathbf{k}'-\mathbf{q}+\mathbf{q}'})(2\omega - \varepsilon^{\nu}_{\mathbf{k}+\mathbf{q}} - \varepsilon^{\nu}_{\mathbf{k}'-\mathbf{q}})} \quad (25)$$

According to a similar procedure in previous papers,[1,3] we study the situation near the extremum (minimum or maximum) of the electron zone. Then we suppose that $\mathbf{k} = \mathbf{k}' = \mathbf{k}_0 + \mathbf{k}''$, and $\varepsilon^{\nu}_{k0} = \varepsilon^{\nu}$ corresponds to the extremum of the zone. We expand the energy in the momentum $\mathbf{k} \pm \mathbf{q}$ in a series up to terms of the second order and suppose that the energy extremum is located near the Fermi-level energy. Then, the sum in the denominator of Eq. (24) is approximately reduced to the following expression:

$$\sum_{\mathbf{q},\mathbf{q}'} K_2(\omega, \mathbf{k}, \mathbf{k}', \mathbf{q}, \mathbf{q}') \approx N(\varepsilon^{\nu}_f) N(\varepsilon^{\nu'}_f) \ln \left| \left(1 - \frac{2\Delta}{a_{\nu'}}\right)\left(1 - \frac{2\Delta}{a_{\nu}}\right) \right| \quad (26)$$

Therefore, we obtain the equation for coupled states in the electron system:

$$1 - g_2^2 N(\varepsilon^{\nu}_f) N(\varepsilon^{\nu'}_f) \ln \left| \left(1 - \frac{2\Delta}{a_{\nu'}}\right)\left(1 - \frac{2\Delta}{a_{\nu}}\right) \right| = 0 \quad (27)$$

From Eq. (27), we find the possibility of the existence of a solution for the coupled states, if $g_2 \neq 0$. Thus, the effective e–e interaction g_2 with a positive value contributes to the superconductivity.

2.5. Cooperative Mechanism

Here, we consider that $g_1 \neq 0$, $g_2 \neq 0$ and others $= 0$. In a similar way, the two-particle Green function (18) is approximately derived as

$$G^{\gamma\delta\beta\sigma}_{2\nu\nu\nu\nu}(\mathbf{p}_3, \mathbf{p}_4, \mathbf{p}_2, \mathbf{k}; t - t') = \frac{f(\mathbf{k}, \mathbf{k}', \omega) \sum_{\sigma,\sigma'} \phi(\sigma, \sigma')}{[1 - (g_1 + g_2) \sum_{\mathbf{q}} K(\omega, \mathbf{k}, \mathbf{k}', \mathbf{q})][1 - (g_1 - g_2) \sum_{\mathbf{q}} K(\omega, \mathbf{k}, \mathbf{k}', \mathbf{q})]} \quad (28)$$

where $K(\omega, \mathbf{k}, \mathbf{k}', \mathbf{q})$ is as given by Eq. (20). The summation in the denominator of Eq. (28) is performed in a similar way, and the equation for coupled states in the electron system is approximately derived as

$$\left[1 - (g_1 + g_2) N(\varepsilon_f) \ln \left| 1 - \frac{\Delta}{a} \right| \right] \times \left[1 - (g_1 - g_2) N(\varepsilon_f) \ln \left| 1 - \frac{\Delta}{a} \right| \right] = 0 \quad (29)$$

When $g_1 + g_2 < 0$ or $g_1 - g_2 < 0$, we can find solutions to this equation.

2.6. Room-Temperature Superconductors

In the previous subsections, we have approximately calculated two-particle Green functions for three cases—traditional superconductivity, copper oxides and the cooperative mechanism—in the framework of a two-band model. From these Green functions, we have derived the equation for coupled states for each case. In the case of a single-band model, which indicates traditional superconductivity such as the BCS theory, it is necessary that the effective e–e interaction be negative ($g_1 < 0$) in order to realize the superconductivity. The maximal transition temperature for the superconductivity predicted by the theory is about 40 K. On the other hand, we can expect, in a two-band model for negative g_1, that the transition temperature becomes higher than that derived within a single-band model, because of the tunneling of Cooper pairs between two bands. The tunneling of Cooper pairs causes stabilization of the order parameter of the superconductivity.[30–32] In the framework of a two-band model, we consider that the Fermi energy level crosses with two bands. The results derived from the two-particle Green function in the previous section suggest that the superconductivity appears for $g_2 < 0$ or $g_2 > 0$. Note that g_2 contributes to SDW. From the results derived from calculations involving g_1 and g_2 (cooperative mechanism), we expect a higher T_c than that of copper oxides.

On the basis of the results obtained in this section, we present a schematic diagram for superconductivity, shown in Figure 2. The mechanism of high-T_c superconductivity of materials such as copper oxides might be around the cooperative mechanism in the figure. In what follows, we calculate a two particle Green function in the two-band model and derive an equation for coupled states. In the framework of the two-band model, the results predict that superconductivity appears even if the e–e interaction is

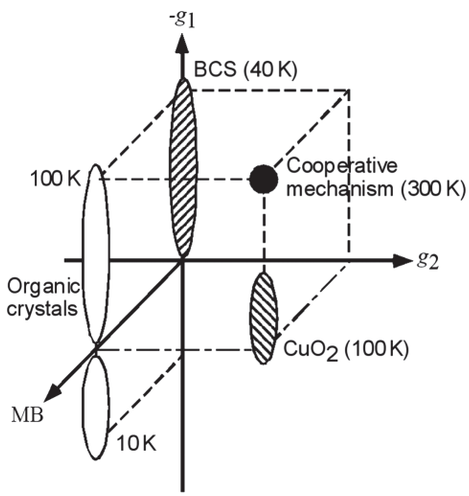

Fig. 2. Schematic diagram for superconductivity. MB means multiband effects.

positive. We can expect that the transition temperature is higher (300 K) than that for copper oxides by the cooperative mechanism.

Let us discuss the problem of superconductors operating at room temperature (RTSCs). It is obvious that the main task in the field of superconductivity is the fabrication of materials with superconducting properties at room temperature. The study of HTSCs is only a stage on the way to the main purpose, namely to the development of RTSCs. At the present time, the highest known $T_c = 135$ K (at the atmospheric pressure). Now there occurs a wide-scale search for such superconductors. Since none of the known physical laws allows one to exclude the possibility for RTSCs to exist, the future discovery of RTSCs seems to be without doubt. New materials are created by means of physical and chemical modifications of the known compounds, including the application of nanotechnological methods. The creation of new materials with preassigned physical properties is one of the actual problems of modern science. At present, various approaches are being developed in order to avoid the labor-consuming sorting of different chemical compounds and conditions of synthesis, i.e., to optimize the solution of this problem. One of the most efficient and promising solution is the method of structural design. In Ref. [33], the structural design was used in solving the problems related to the search for new HTSCs on the basis of complex copper oxides.

We now present the recommendations concerning the search for new HTSCs with higher critical temperatures which were advanced by the Nobel Prize winner Müller.[34] He divided the well-known HTSCs into three classes:

(1) Layered cuprates,
(2) MgB_2,
(3) Doped fullerenes of the type K_3C_{60}.

Müller emphasizes that the discovery of cuprate superconductors was promoted by the concept of Jahn–Teller polarons. Two singlet polarons form a bipolaron. Bipolarons are able, in turn, to form metallic clusters (stripes). Müller indicated the following factors which should be taken into account in the search for new HTSCs:

(1) Superconductivity is favored by a layered (quasi-two-dimensional) crystalline structure;
(2) Oxygen ions are proposed as anions;
(3) Fluorine, chlorine and nitrogen can be considered as well.

It is worth noting that the recent discovery of FeAs superconductors eliminated the monopoly of cuprates in the physics of HTSCs. It is possible that new superconductors should be sought in the other rows and columns of the periodic table. It is necessary to concentrate efforts on the purposeful search for and the creation of new HTSCs.

3. TWO-GAP SUPERCONDUCTIVITY IN MgB_2

3.1. The Physical Properties of MgB_2

Recently, the superconductivity of MgB_2 with $T_c = 39$ K, which is the highest temperature among two-component systems, was discovered.[35] The great interest in the study of magnesium diboride is related to the fact that MgB_2 has occupied the "intermediate" place between low- and high-temperature superconductors by the value of T_c. Therefore, modern literature calls MgB_2 a "medium-T_c superconductor" (MTSC). The low cost of this superconductor also makes it economical for use. We recall that wires made of cuprate superconductors include 70% of silver, which is expensive. An important peculiarity of MgB_2 is its quasi-two-dimensional structure of the AlB_2 type. Interestingly, AlB_2 is not superconducting. Note that MgB_2 is another example of the crucial role played by the lattice structure regarding superconductivity.[36] It is an "old" material which has been known since the early 1950s, but only recently discovered to be superconducting. MgB_2 has a hexagonal structure;[37] see Figure 4.[38] The results of calculations of the temperature dependence of the specific heat of MgB_2 given in Figure 5 follow the corresponding experimental data. The band structure of MgB_2 has been calculated in several works since the discovery of superconductivity.[39] The electronic properties of MgB_2 are plotted in Figure 3. The band structure of MgB_2 is similar to that of graphite and is formed by the σ and π zones.

The important problem for superconductivity in MgB_2 is the mechanism of superconductivity. It can be the conventional electron-phonon (e-p) mechanism or a more exotic mechanism. The presence of an isotope effect is a strong indicator of the phonon mediation of superconductivity. The large isotope effect $\alpha_B = 0.26$[40] shows that phonons associated with B vibrations play a significant role in the MgB_2 superconductivity, whereas the magnesium isotope effect is very small: $\alpha_M = 0.02$.[40] The total isotope effect is

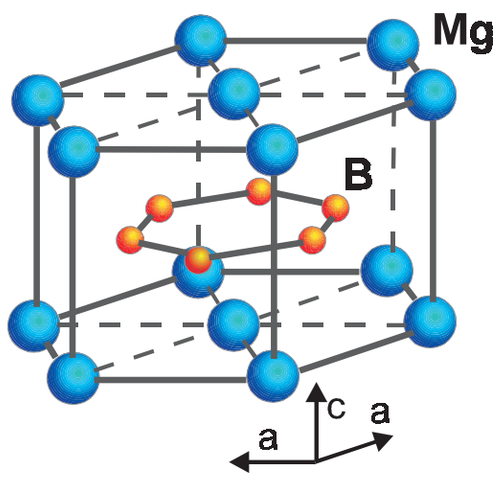

Fig. 3. The structure of MgB_2 containing graphite-type B layers separated by hexagonal close-packed layers of Mg.

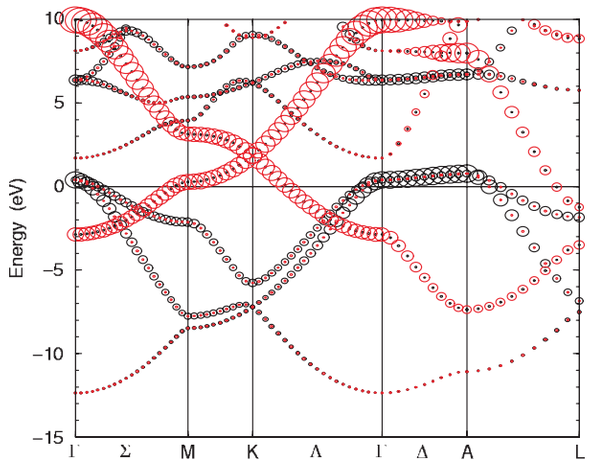

Fig. 4. Band structure of MgB_2.

$\alpha_B + \alpha_M = 0.3$, which supports the electron-phonon mechanism of superconductivity.

MgB_2 is a II-type superconductor.[36] The discovery of the superconductivity of MgB_2 has aroused great interest in multigap superconductivity.[40] MgB_2 has two superconducting gaps, 4 meV and 7.5 meV, due to the π and σ electron bands. The two-gap structure was established in a number of experiments.[41] The plot of the specific heat of MgB_2 versus temperature (Fig. 5) demonstrates good agreement between the theoretical and experimental data. Both gaps have s symmetry and result from the highly anisotropic layer structure of MgB_2. Although multigap superconductivity was discussed theoretically[30–32] as early as 1958, it was only observed experimentally[42] in the 1980s. MgB_2 is the first material in which the effects of multigap superconductivity are so dominant, and its implications so thoroughly explored. Recent band calculations[39, 43] of MgB_2 with the McMillan formula for the transition temperature have supported the e-p interaction mechanism for the superconductivity. In this case, the possibility of two-band superconductivity has also been discussed in relation to two-gap functions experimentally and theoretically. Very recently, two-band or multiband superconductivity has been theoretically investigated in relation to the superconductivity arising from Coulomb repulsive interactions. The two-band model was introduced by Kondo.[32] We have also investigated anomalous phases in the two-band model by using the Green function techniques.[1–4, 6, 8] Recently, we have pointed out the importance of multiband effects in high-T_c superconductivity.[1–3] The expressions for the transition temperature for several phases have been derived, and the approach has been applied to the superconductivity in molecular crystals by charge injection and the field-induced superconductivity.[24] In previous papers,[1–4, 6, 8] we have investigated the superconductivity by using the two-band model and the two-particle Green function techniques. We have applied the model to the e-p mechanism for the traditional BCS method, the e–e interaction mechanism for high-T_c superconductivity,[13] and the cooperative mechanism. In the framework of the two-particle Green function techniques,[6] it has been shown that the temperature dependence of the superconductivity gap for high-T_c superconductors is more complicated than that predicted in the BCS approach. In Ref. [4], phase diagrams for the two-band model superconductivity have been investigated, by using the renormalization group approach. Below, we will discuss the possibility of the cooperative mechanism of two-band superconductivity in relation to high-T_c superconductivity and study the effect of the increase of T_c in MgB_2 due to the enhanced interband pairing scattering. In this section, we will investigate our two-band model for the explanation of the multigap superconductivity of MgB_2. We apply the model to the e-p mechanism for the traditional BCS method, the e–e interaction mechanism for high-T_c superconductivity, and the cooperative mechanism in relation to multiband superconductivity.

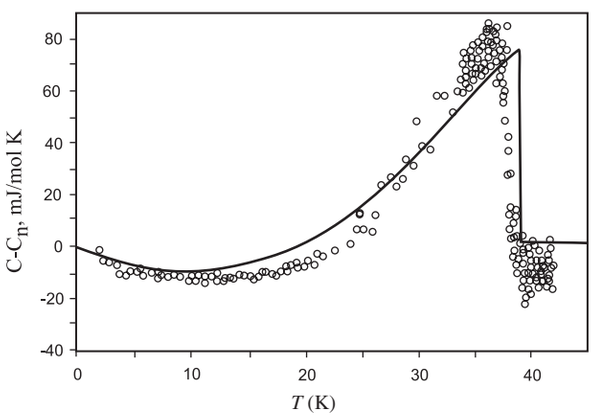

Fig. 5. The MgB_2 specific heat versus temperature. The line indicates theory, and the circles represent the experimental data.

3.1.1. $Mg_{1-x}Al_xB_2$

Critical temperature and other superconducting properties of two-band superconductors depend on the doping level as well as the interband and intraband scattering, which can be modified by chemical substitutions. The influence of doping on the transition temperature in $Mg_{1-x}Al_xB_2$ is illustrated in Figure 6. It is seen that the doping destroys the superconductivity in MgB_2. This can be understood as a result of the competition of two effects: the first one is a coupling effect related to the changes of the carrier concentration, and the second one depends on the introduction of new scattering centers leading to a modification of the interband and intraband scattering.

3.2. Theoretical Model

In this subsection, we will use the two-band model for superconductivity. We start from the Hamiltonian for two bands i and j:

$$H = H_0 + H_{\text{int}} \tag{30}$$

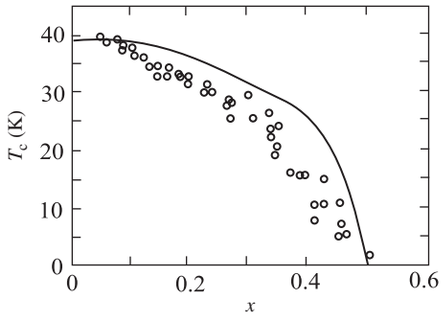

Fig. 6. The influence of doping on T_c in $Mg_{1-x}Al_xB_2$. The line indicates theory, and the circles represent the experimental data.

with

$$H_0 = \sum_{\mathbf{k},\sigma}[[\epsilon_i(\mathbf{k}) - \mu]a^\dagger_{i\mathbf{k}\sigma}a_{i\mathbf{k}\sigma} + [\epsilon_j(\mathbf{k}) - \mu]a^\dagger_{j\mathbf{k}\sigma}a_{j\mathbf{k}\sigma}] \quad (31)$$

$$\begin{aligned} H_{\text{int}} = \frac{1}{4}\sum_{\delta(\mathbf{p}_1+\mathbf{p}_2,\,\mathbf{p}_3+\mathbf{p}_4)}\sum_{\alpha,\beta,\gamma,\delta}[&\Gamma^{iiii}_{\alpha\beta\gamma\delta}a^\dagger_{i\mathbf{p}_1\alpha}a^\dagger_{i\mathbf{p}_2\beta}a_{i\mathbf{p}_3\gamma}a_{i\mathbf{p}_4\delta} \\ &+ (i \leftrightarrow j) + \Gamma^{iijj}_{\alpha\beta\gamma\delta}a^\dagger_{i\mathbf{p}_1\alpha}a^\dagger_{i\mathbf{p}_2\beta}a_{j\mathbf{p}_3\gamma}a_{j\mathbf{p}_4\delta} + (i \leftrightarrow j) \\ &+ \Gamma^{ijij}_{\alpha\beta\gamma\delta}a^\dagger_{i\mathbf{p}_1\alpha}a^\dagger_{j\mathbf{p}_2\beta}a_{i\mathbf{p}_3\gamma}a_{j\mathbf{p}_4\delta} + (i \leftrightarrow j)] \end{aligned} \quad (32)$$

where Γ is the bare vertex part,

$$\begin{aligned} \Gamma^{ijkl}_{\alpha\beta\gamma\delta} = &\langle i\mathbf{p}_1\alpha j\mathbf{p}_2\beta \mid k\mathbf{p}_3\gamma l\mathbf{p}_4\delta\rangle\delta_{\alpha\delta}\delta_{\beta\gamma} \\ &- \langle i\mathbf{p}_1\alpha j\mathbf{p}_2\beta \mid l\mathbf{p}_4\delta k\mathbf{p}_3\gamma\rangle\delta_{\alpha\gamma}\delta_{\beta\delta} \end{aligned} \quad (33)$$

with

$$\begin{aligned} &\langle i\mathbf{p}_1\alpha j\mathbf{p}_2\beta \mid k\mathbf{p}_3\beta l\mathbf{p}_4\alpha\rangle \\ &= \int dr_1 dr_2 \phi^*_{i\mathbf{p}_1\alpha}(r_1)\phi^*_{j\mathbf{p}_2\beta}(r_2)V(r_1, r_2) \\ &\times \phi_{k\mathbf{p}_3\beta}(r_2)\phi_{l\mathbf{p}_4\alpha}(r_1) \end{aligned} \quad (34)$$

where $a_{i\mathbf{p}\sigma^+}$ ($a_{i\mathbf{p}\sigma}$) is the creation (annihilation) operator corresponding to the excitation of electrons (or holes) in the ith band with spin σ and momentum $\mathbf{p}$, μ is the chemical potential and ϕ is a single-particle wave function. Here, we suppose that the vertex function in Eq. (56) involves the effective interactions between the carriers caused by the linear vibronic coupling in several bands and the screened Coulombic interband interaction of carriers.

When we use the two-band Hamiltonian (1) and define the order parameters for a singlet exciton, triplet exciton and singlet Cooper pair, the mean field Hamiltonian is easily derived.[1–4, 6, 8] Here, we focus on three electron scattering processes contributing to the singlet superconducting phase in the Hamiltonian ((1):

$$g_{i1} = \langle ii \mid ii\rangle, \quad g_{j1} = \langle jj \mid jj\rangle \quad (35)$$

$$g_2 = \langle ii \mid jj\rangle = \langle jj \mid ii\rangle \quad (36)$$

$$g_3 = \langle ij \mid ij\rangle = \langle ji \mid ji\rangle \quad (37)$$

$$g_4 = \langle ij \mid ji\rangle = \langle ji \mid ij\rangle \quad (38)$$

where g_{i1} and g_{j1} represent the ith and jth intraband two-particle normal scattering processes, respectively, and g_2 indicates the intraband two particle umklapp scattering (see Fig. 7). For simplicity, we consider the three cases in Refs. [4, 5]:

(i) $g_1 \neq 0$ and others $= 0$;

(ii) $g_2 \neq 0$; and others $= 0$;

(iii) g_{i1} and g_{j1}, and others $= 0$, using the two-particle Green function techniques (see Fig. 7).

It was shown that, possibly, the two-gap superconductivity arises in case (iii). The superconductivity arising from the e-p mechanism ($g_1 < 0$ and $g_1 < g_2$) such as for MgB_2 is in the two-gap region. On the other hand, the superconductivity of copper oxides ($g_1 > g_2$) is outside the two-gap region. These results predict that we may observe two-gap functions for MgB_2 and only a single-gap function for copper oxides.

3.3. Superconductivity in MgB_2

Using case (iii) for g_{i1} and g_{j1}, $g_2 \neq 0$ and others = 0 to describe the superconductivity in MgB_2. We now have a reduced Hamiltonian:

$$H = H_0 + H_{\text{int}} \quad (39)$$

where

$$H_0 = \sum_{\mathbf{k},\,\sigma}[[\epsilon_i - \mu]a^\dagger_{i\mathbf{k}\sigma}a_{i\mathbf{k}\sigma} + [\epsilon_j - \mu]a^\dagger_{j\mathbf{k}\sigma}a_{j\mathbf{k}\sigma}] \quad (40)$$

$$\begin{aligned} H_{\text{int}} = &\sum g_{1i}a^\dagger_{i\mathbf{k}}a^\dagger_{i-\mathbf{k}}a_{i-\mathbf{k}}a_{i\mathbf{k}} + \sum i \rightarrow j \\ &+ \sum g_2 a^\dagger_{i\mathbf{k}}a^\dagger_{i-\mathbf{k}}a_{j-\mathbf{k}}a_{j\mathbf{k}} \end{aligned} \quad (41)$$

We now define the order parameters which are helpful in constructing the mean-field Hamiltonian:

$$\Delta_i = \sum_p \langle a^\dagger_{ip\uparrow}a^\dagger_{i-p\downarrow}\rangle \quad (42)$$

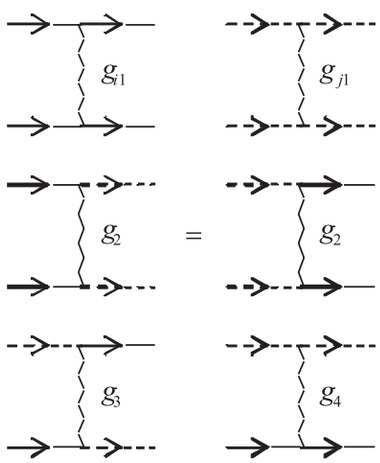

Fig. 7. Electron–electron interactions. Solid and dashed lines indicate π and σ bands, respectively; g_{i1}, g_{j1}, g_2 and g_4 contribute to superconductivity.

$$\Delta_j = \sum_p \langle a^{\dagger}_{jp\uparrow} a^{\dagger}_{j-p\downarrow} \rangle \tag{43}$$

The relation between two superconducting gaps of the system is as follows:

$$\Delta_j = \frac{1 - g_{i1}\rho_i f_i}{g_2 \rho_j f_j}\Delta_i \tag{44}$$

where

$$\begin{aligned} f_i &= \int_{\mu}^{\mu - E_c} \frac{d\xi}{(\xi^2 + \Delta_i^2)^{1/2}} \tanh \frac{(\xi^2 + \Delta_i^2)^{1/2}}{2T} \\ f_j &= \int_{\mu - E_c}^{\mu - E_j} \frac{d\xi}{(\xi^2 + \Delta_j^2)^{1/2}} \tanh \frac{(\xi^2 + \Delta_j^2)^{1/2}}{2T} \end{aligned} \tag{45}$$

with the coupled gap equation

$$(1 - g_{i1}\rho_i f_i)(1 - g_{j1}\rho_j f_j) = g_2^2 f_i f_j \tag{46}$$

We have tried to estimate the coupling constant of the pair electron scattering process between the π and σ bands of MgB_2 and have calculated the parameters by using a rough numerical approximation. We focus on one π band and σ band of MgB_2 and consider electrons near Fermi surfaces. We found that the parameter $g_1 = -0.4$ eV, by using the transfer integral between the ð and ó bands. We estimate the coupling parameter g_2 of the pair electron scattering process by the expression

$$g_2 = \sum_{k1,k2} V^{1,2}_{k1,k2} \tag{47}$$

$$V^{1,2}_{k1,k2} = \sum_{r,s,t,u} u^*_{1,r}(k1) u^*_{1,s}(k1) v_{rs} u_{2,t}(k2) u_{2,u}(k2) \tag{48}$$

where the labels 1 and 2 are the π band and the σ band, respectively, $u_{i,r}(\xi)$ is the LCAO coefficient for the ith band and ξ is the moment.[25,26] The indices $k1$ and $k2$ are summed over each Fermi surface. However, it is difficult to perform the sum exactly. In this case, we used a few points near the Fermi surface. The coupling constant of the pair electron scattering between the π band and the σ band is $g_2 = 0.025$ eV. From numerical calculations of Eqs. (53)–(53), we can also obtain the temperature dependence of the two-gap parameters (see Fig. 8). We have used the density of states of the π and σ bands ($\rho_i = 0.2$ eV^{-1}, $\rho_j = 0.14$ eV^{-1}), chemical potential $\mu = -2.0$, the top energy of the σ band $E_j = -1.0$ and the fitting parameters ($g_{i1} = -0.4$ eV, $g_{j1} = -0.6$ eV, $g_2 = 0.02$ eV). These calculations have qualitative agreement with experiments.[37,41,44] The expression for the transition temperature of superconductivity derived in a simple approximation is:

$$T_{c_+} = 1.13(\zeta - E_j) \cdot \exp\left(\frac{-1}{g_+ \rho}\right) \tag{49}$$

where

$$g_+ = \frac{1}{24}(B + \sqrt{B^2 - 4A}) \tag{50}$$

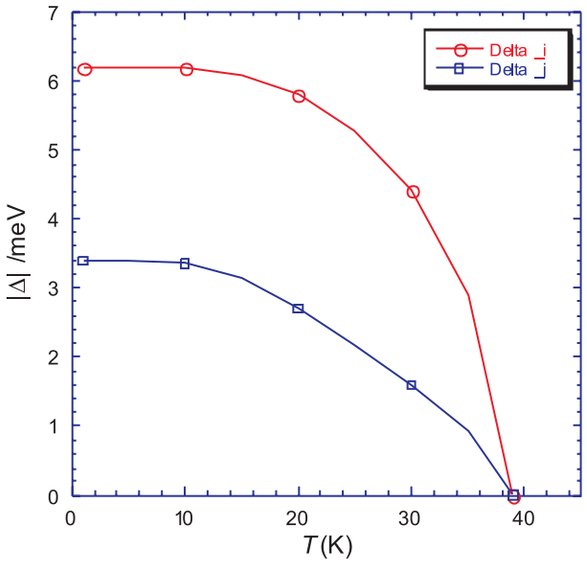

Fig. 8. Electron–electron interactions. Solid and dashed lines indicate π and σ bands, respectively; g_{i1}, g_{j1}, g_2 and g_4 contribute to superconductivity.

and

$$A = g_{1i} g_{1j} - g_2^2 \tag{51}$$

$$B = g_{1i} + g_{1j} \tag{52}$$

$$\zeta = -\mu \tag{53}$$

From the expressions for T_{c+}, we can see the effect of increase of T_{c+} due to the enhanced interband pairing scattering (g_2).

Figure 9 shows a schematic diagram of the mechanism of pairing for two gaps. The scenario is as follows. Electrons from the π and σ bands make up the subsystems. For g_2, we have two independent subsystems with the different transition temperatures of superconductivity $T_{c\pi}$ and $T_{c\sigma}$ and two independent superconducting gaps. In our model, we have two coupled superconducting gaps with the relation (53) and one transition temperature of superconductivity T_{c+}, which is in agreement with experiments. In this model, we have two channels of superconductivity: conventional channel (intraband g_1) and unconventional channel (interband g_2). Two gaps appear simultaneously in different bands which are like BCS gaps. The gap in the π band is bigger than that for the σ band, because the density of state is 0.25 eV in the π band and 0.14 eV in

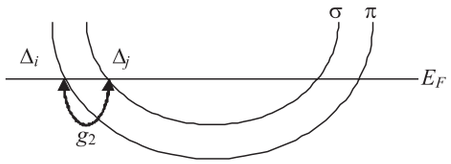

Fig. 9. Schematic diagram of the mechanism of pairing for two gaps.

the σ band. The current of Cooper pairs flows from the π band into the σ band, because the density of Cooper pairs in the π band is much higher. The tunneling of Cooper pairs also stabilizes the order parameter in the σ band. In this way, we can predict the physical properties of the multigap superconductivity if we have the superconductors with a multiband structure, as shown in Figure 9.

Thus, we have presented our two-band model with the intraband two-particle scattering and interband pairing scattering processes to describe two-gap superconductivity in MgB_2. We defined the parameters of our model and made numerical calculations of the temperature dependence of two gaps in qualitative agreement with experiments. We have proposed a two-channel scenario of superconductivity: the conventional channel (intraband g_1), which is connected with the BCS mechanism in different bands; and the unconventional channel (interband g_2), which describes the tunneling of Cooper pairs between two bands. The tunneling of Cooper pairs also stabilizes the order parameters of superconductivity and increases the critical temperature of superconductivity.

4. THEORETICAL STUDIES OF MULTIBAND EFFECTS IN SUPERCONDUCTIVITY BY USING THE RENORMALIZATION GROUP APPROACH

We present the renormalization equations using the two-band model and construct phase diagrams for the two-band superconductivity. In the framework of the two-band model, the given results predict that superconductivity appears, even if the e–e interaction is positive. We discuss the possibility of a cooperative mechanism in the two-band superconductivity in relation to high-T_c superconductivity. The recent discovery of superconductivity in MgB_2[35] has also attracted great interest to the elucidation of its mechanism from both the experimental and theoretical viewpoints. A crucial role of the e-p interaction has been pointed out for the superconductivity of MgB_2. Recent band calculations of the transition temperature for MgB_2[39,43] with the McMillan formula[45] have supported the e-p interaction mechanism for the superconductivity. In this case, the possibility of the two-band superconductivity in relation to two-gap functions has also been considered experimentally and theoretically. Very recently, the two-band or multiband superconductivity has been theoretically investigated in relation to the superconductivity arising from Coulomb repulsive interactions.[32] The two-band model was introduced by Kondo.[32] Recently, we have pointed out the importance of multiband effects in high-T_c superconductivity.[4,46] We have also investigated anomalous phases in the two-band model by using the Green function techniques.[6,47] The expressions of the transition temperature for several phases have been derived, and the approach has been applied to the superconductivity in several crystals by charge injection and the field-induced superconductivity.[47,48] In the previous section, we have investigated superconductivity by using the two-band model and the two-particle Green function techniques.[4,6] We have applied the model to the e-p mechanism for the traditional BSC method, the e–e interaction mechanism for high-T_c superconductivity and the cooperative mechanism. In the framework of the two-particle Green function techniques,[8] it has been shown that, in the e-p system, a class of new so-called coupled states arises. In this section, we investigate two- or multiband effects in superconductivity by using the two-band model within the renormalization group approach. Renormalization equations for the two-band superconductivity are derived from the response function and the vertex correction of the model. Phase diagrams numerically obtained from the renormalization equations are presented. We also discuss the superconductivity arising from the e–e repulsive interaction in relation to the two-band superconductivity.

4.1. Theoretical Model

In this subsection, we summarize the two-band model for the superconductivity and introduce the renormalization group approach.[49,50]

We consider a Hamiltonian for two bands i and j, written as

$$H = H_0 + H_{\text{int}} \tag{54}$$

with

$$H_0 = \sum_{\mathbf{k},\sigma} [[\epsilon_i(\mathbf{k}) - \mu] a^\dagger_{i\mathbf{k}\sigma} a_{i\mathbf{k}\sigma} + [\epsilon_j(\mathbf{k}) - \mu] a^\dagger_{j\mathbf{k}\sigma} a_{j\mathbf{k}\sigma}] \tag{55}$$

$$\begin{aligned} H_{\text{int}} = \frac{1}{4} \sum_{\delta(\mathbf{p}_1+\mathbf{p}_2,\mathbf{p}_3+\mathbf{p}_4)} \sum_{\alpha,\beta,\gamma,\delta} & [\Gamma^{iiii}_{\alpha\beta\gamma\delta} a^\dagger_{i\mathbf{p}_1\alpha} a^\dagger_{i\mathbf{p}_2\beta} a_{i\mathbf{p}_3\gamma} a_{i\mathbf{p}_4\delta} \\ & + (i \leftrightarrow j) + \Gamma^{iijj}_{\alpha\beta\gamma\delta} a^\dagger_{i\mathbf{p}_1\alpha} a^\dagger_{i\mathbf{p}_2\beta} a_{j\mathbf{p}_3\gamma} a_{j\mathbf{p}_4\delta} + (i \leftrightarrow j) \\ & + \Gamma^{ijij}_{\alpha\beta\gamma\delta} a^\dagger_{i\mathbf{p}_1\alpha} a^\dagger_{j\mathbf{p}_2\beta} a_{i\mathbf{p}_3\gamma} a_{j\mathbf{p}_4\delta} + (i \leftrightarrow j)] \end{aligned} \tag{56}$$

where Γ is the bare vertex part,

$$\begin{aligned} \Gamma^{ijkl}_{\alpha\beta\gamma\delta} = & \langle i\mathbf{p}_1\alpha j\mathbf{p}_2\beta \mid k\mathbf{p}_3\gamma l\mathbf{p}_4\delta\rangle \delta_{\alpha\delta}\delta_{\beta\gamma} \\ & - \langle i\mathbf{p}_1\alpha j\mathbf{p}_2\beta \mid l\mathbf{p}_4\delta k\mathbf{p}_3\gamma\rangle \delta_{\alpha\gamma}\delta_{\beta\delta} \end{aligned} \tag{57}$$

with

$$\begin{aligned} & \langle i\mathbf{p}_1\alpha j\mathbf{p}_2\beta \mid k\mathbf{p}_3\beta l\mathbf{p}_4\alpha\rangle \\ & = \int dr_1 dr_2 \phi^*_{i\mathbf{p}_1\alpha}(r_1)\phi^*_{j\mathbf{p}_2\beta}(r_2) V(r_1, r_2) \\ & \quad \times \phi_{k\mathbf{p}_3\beta}(r_2)\phi_{l\mathbf{p}_4\alpha}(r_1) \end{aligned} \tag{58}$$

where $a^\dagger_{i\mathbf{p}\sigma}(a_{i\mathbf{p}\sigma})$ is the creation (annihilation) operator corresponding to the excitation of electrons (or holes) in the ith band with spin σ and momentum $\mathbf{p}$, μ is the chemical potential and $\phi^*_{i\alpha\mathbf{p}_1}$ is a single-particle wave function. Here, we suppose that the vertex function in Eq. (56)

involves the effective interactions between carriers caused by the linear vibronic coupling in several bands and the screened Coulombic interband interaction of carriers.

We focus on three electron scattering processes contributing to the singlet superconducting phase in the Hamiltonian (56), as shown in Figure 10:

$$g_{i1} = \langle ii \mid ii \rangle \tag{59}$$

$$g_{j1} = \langle jj \mid jj \rangle \tag{60}$$

$$g_2 = \langle ii \mid jj \rangle = \langle jj \mid ii \rangle \tag{61}$$

where g_{i1} and g_{j1} represent the ith and jth intraband two-particle normal scattering processes, respectively, and g_2 indicates the intraband two-particle umklapp scattering. Note that the Γ's are given by

$$\begin{aligned}
\Gamma^{iiii}_{\alpha\beta\gamma\delta} &= g_{i1}(\delta_{\alpha\delta}\delta_{\beta\gamma} - \delta_{\alpha\gamma}\delta_{\beta\delta}) \\
\Gamma^{jjjj}_{\alpha\beta\gamma\delta} &= g_{j1}(\delta_{\alpha\delta}\delta_{\beta\gamma} - \delta_{\alpha\gamma}\delta_{\beta\delta}) \\
\Gamma^{iijj}_{\alpha\beta\gamma\delta} = \Gamma^{jjii}_{\alpha\beta\gamma\delta} &= g_2(\delta_{\alpha\delta}\delta_{\beta\gamma} - \delta_{\alpha\gamma}\delta_{\beta\delta})
\end{aligned} \tag{62}$$

where we assume that an antisymmetrized vertex function Γ is a constant independent of the momenta.

The spectrum is elucidated by the Green function method. Using Green functions which characterize the CDW, SDW and SSC phases, we obtain a self-consistent equation according to the traditional procedure.[25, 46, 47, 51–53] Then we can obtain expressions for the transition temperature in some cases. Electronic phases of a one-dimensional system have been investigated by using a similar approximation in the framework of the one-band model.[50–53] In the framework of the mean-field approximation within the two-band model, we have already derived expressions for the transition temperature for CDW, SDW and SSC. In Refs. [47, 46], we have investigated the dependence of T_c on the hole or electron concentration for the superconductivity of copper oxides by using the two-band model and have obtained a phase diagram of $Bi_2Sr_2Ca_{1-x}Y_xCu_2O_8$ (Bi-2212) by means of the above expressions for the transition temperature.

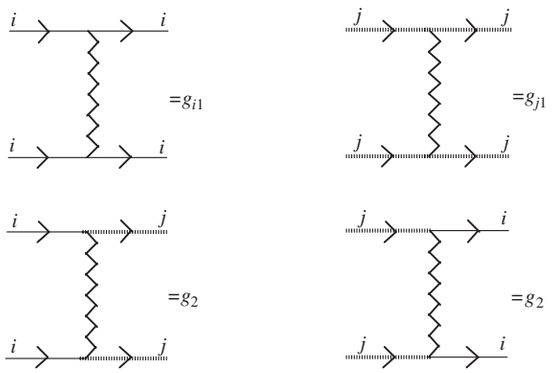

Fig. 10. Electron–electron interactions. Dependence of g on the direction in the momentum space is ignored in this model [$g_x(\mathbf{k}) \approx g_x$ ($x = i, j$)]. We assume that g_x is constant.

4.2. Renormalization-Group Approach

The Dyson equation is invariant under a multiple renormalization of Green function and coupling parameters g. From this invariance for a scaling procedure, we obtain differential equations for the coupling parameters and the external vertex of a Cooper pair:

$$y\frac{\partial}{\partial y}\tilde{g}_i(y,u,g) = \frac{\partial}{\partial \xi}\tilde{g}_i\left(\xi, \frac{u}{y}, \tilde{g}(t,u,g)\right)\Big|_{\xi=1} \tag{63}$$

$$y\frac{\partial}{\partial y}\ln\Lambda(y,u,g) = \frac{\partial}{\partial \xi}\ln\Lambda\left(\xi, \frac{u}{y}, \tilde{g}(t,u,g)\right)\Big|_{\xi=1} \tag{64}$$

where y and u are parameters with the dimension of energy, g is the set of original couplings and Λ is the external vertex.

4.3. Vertex Correction and Response Function for Cooper Pairs

To solve Eqs. (63) and (64), we estimate the right-hand side of Eq. (63) by using the perturbation theory. We consider the lowest-order correction to the vertex for a Cooper pair, as shown in Figure 11. From these diagrams, we obtain

$$\begin{pmatrix} \tilde{g}_{i1} \\ \tilde{g}_{j1} \end{pmatrix} = \begin{pmatrix} g_{i1} \\ g_{j1} \end{pmatrix} + \begin{pmatrix} -g_{i1}^2 & -g_2^2 \\ -g_{j1}^2 & -g_2^2 \end{pmatrix} \begin{pmatrix} L_i \\ L_j \end{pmatrix} \tag{65}$$

$$\begin{pmatrix} \tilde{g}_2 \\ \tilde{g}_2 \end{pmatrix} = \begin{pmatrix} g_2 \\ g_2 \end{pmatrix} + \begin{pmatrix} -g_{i1}g_2 & -g_2g_{j1} \\ -g_{j1}g_2 & -g_2g_{i1} \end{pmatrix} \begin{pmatrix} L_i \\ L_j \end{pmatrix} \tag{66}$$

with

$$\begin{aligned}
L_i = \Pi_i(\mathbf{k},\omega) &= \frac{T}{N}\sum_{\mathbf{q},\omega'} G_i(\mathbf{q},\omega')G_i(\mathbf{k}-\mathbf{q},\omega-\omega') \\
L_j = \Pi_j(\mathbf{k},\omega) &= \frac{T}{N}\sum_{\mathbf{q},\omega'} G_j(\mathbf{q},\omega')G_j(\mathbf{k}-\mathbf{q},\omega-\omega')
\end{aligned} \tag{67}$$

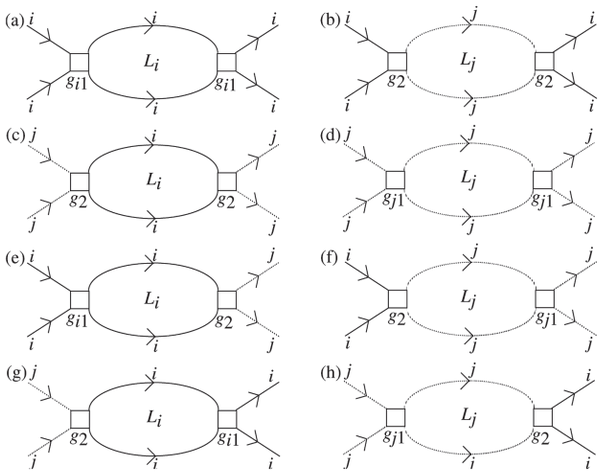

Fig. 11. Diagrams of the first-order vertex correction. (a) and (b) contribute to $\tilde{g}_{i1}$, (c) and (d) are diagrams for $\tilde{g}j1$, and (e)–(h) for $\tilde{g}_2$.

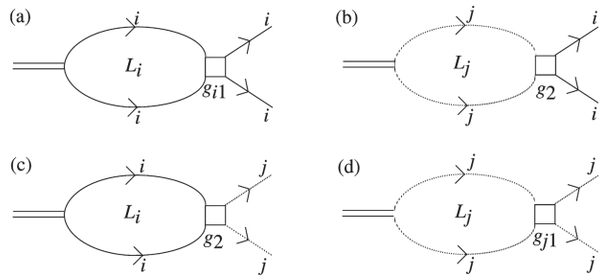

Fig. 12. Diagrams of the first-order response function. (a) and (b) contribute to Λ_i, and (c) and (d) show diagrams for Λ_j.

where G and T are the temperature Green function and temperature, respectively. For the special case $\omega = 0$, $\mathbf{k} = 0$, the functions L_i and L_j become

$$L_i = -\left[\tanh\left(\frac{u_i/y}{2\xi}\right) + \tanh\left(\frac{u_i'/y}{2\xi}\right)\right]\ln\xi - 2A \tag{68}$$

$$L_j = -\left[\tanh\left(\frac{u_j/y}{2\xi}\right) + \tanh\left(\frac{u_j'/y}{2\xi}\right)\right]\ln\xi - 2A \tag{69}$$

where

$$A = \int dx \ln x \operatorname{sech}^2 x \tag{70}$$

u_i (u_j) and u_i' (u_j') are dimensionless functions expressed by the chemical potential, the cutoff energy, the top energy of the jth band, and the density of state for the ith (jth) band.

Next, we consider a first-order response function for a singlet Cooper pair, as shown in Figure 12. Then the first-order vertex function Λ for the ith and jth bands can be written as

$$\begin{pmatrix}\Lambda_i + \Lambda_j \\ \Lambda_i - \Lambda_j\end{pmatrix} = \begin{pmatrix}2 \\ 0\end{pmatrix} + \begin{pmatrix}-g_1 & -g_2 \\ -g_1 & g_2\end{pmatrix}\begin{pmatrix}L_i + L_j \\ L_i - L_j\end{pmatrix} \tag{71}$$

4.4. Renormalization Equation

For simplicity, we hereafter assume that $g_{i1} = g_{j1}$. From Eqs. (63), (65), and (66), we obtain the differential equations written as

$$\frac{\partial}{\partial x}\tilde{g}_1 = -(\tilde{g}_1^2 + \tilde{g}_2^2) \tag{72}$$

$$\frac{\partial}{\partial x}\tilde{g}_2 = -2\tilde{g}_1\tilde{g}_2 \tag{73}$$

In a similar way, using Eqs. (64) and (71), we obtain the differential equations written as

$$\frac{\partial}{\partial x}\ln\Lambda_+ = -\tilde{g}_1 - \tilde{g}_2 \tag{74}$$

$$\frac{\partial}{\partial x}\ln\Lambda_- = -\tilde{g}_1 + \tilde{g}_2 \tag{75}$$

where $\Lambda_+ = \Lambda_i + \Lambda_j$ and $\Lambda_- = \Lambda_i - \Lambda_j$.

4.5. Phase Diagrams

In the previous subsection, we have derived the basic Eqs. (72)–(75) to find the low-temperature phases. For the special case of $g_2 = 0$, we obtain an analytic solution:

$$\tilde{g}_1 = \frac{1}{x + g_1^{-1}} \tag{76}$$

$$\tilde{g}_2 = 0 \tag{77}$$

$$\Lambda_i = \Lambda_j = \frac{1}{g_1 x + 1} \tag{78}$$

From these solutions, we find that the superconducting phase appears only when the intraband interaction g_1 is negative. In the case of the traditional superconductivity described by the BCS theory, it is necessary that the effective e–e interaction be negative ($g_1 < 0$) in order to realize the superconductivity. The present result agrees with that

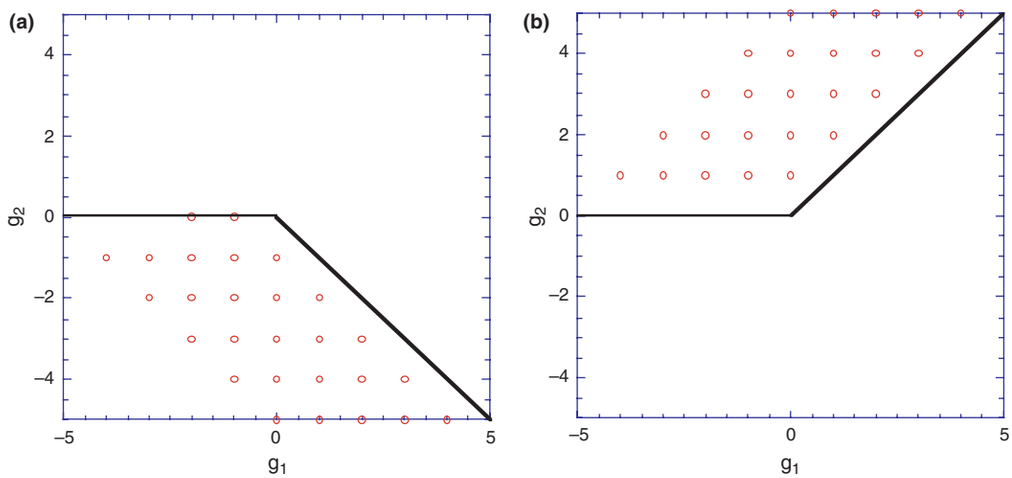

Fig. 13. Phase diagrams for superconductivity: (a) $\Lambda_i + \Lambda_j$, (b) $\Lambda_i - \Lambda_j$.

of the traditional theory for superconductivity expressed by the one-band model. For the case of $g_2 \neq 0$, the phase diagrams numerically obtained from the above renormalization equations are shown in Figure 13. Figure 13(a) shows the phase diagram for the sum of contributions to the superconductivity from the ith and jth bands. Thus, this phase implies that the signs of the superconducting state for the ith and jth bands are the same. From this diagram, we find the superconductivity only for $-g_1 - g_2 > 0$, with negative g_2. On the other hand, the phase diagram for the difference between the superconducting states for the ith and jth bands is shown in Figure 13(b). In this case, this phase means that the sign of the superconductivity for the ith band is different from that of the jth band. We can see that the superconductivity appears only for $-g_1 + g_2 > 0$ with positive g_2 from Figure 13(b). Thus, the present results suggest that the two-band superconductivity appears when the intraband umklapp repulsive scattering g_2 is larger than the normal repulsive scattering g_1. In the region of $g_2 > g_1$ with $g_2 < 0$ and $g_2 < -g_1$ with $g_2 > 0$ (two-gap region), we can expect that two-gap functions are observed. In the former region, those superconducting gaps may be expressed by $|\Lambda_+| > |\Lambda_-|$, and the latter may be $|\Lambda_+| < |\Lambda_-|$. On the other hand, we expect only a single-gap function in the other region. These results agree with the previous solutions[1,4] derived by using the two-particle Green function techniques. The superconductivity arising from the e-p mechanism ($g_1 < 0$ and $|g_2| < |g_1|$) such as that in MgB_2 is in the two-gap region. On the other hand, the superconductivity such as in copper oxides ($|g_2| > |g_1|$) is outside the two-gap region. These results predict that we may observe two-gap functions for MgB_2 and only a single-gap function for copper oxides. In the two-band model for negative g_1 with transferring or tunneling of Cooper pairs between two bands, we can expect that the transition temperature becomes higher than that derived from the single band model. The tunneling of Cooper pairs causes stabilization of the order parameter of superconductivity.[30–32] We can also expect higher T_c of the superconductivity than that for copper oxides in two regions ($g_1 < 0$, $g_2 < 0$ and $g_1 < 0$, $g_2 > 0$) by the cooperative mechanism. Phase diagrams for CDW, SDW, and singlet superconductivity derived from a more general Hamiltonian will be presented elsewhere.

Thus, we have derived the renormalization equations and presented the phase diagrams for the two-band superconductivity. In the framework of the two-band model, the present results predict that superconductivity appears even if the e–e interaction is positive. We can expect that the transition temperature becomes higher than that of copper oxides by the cooperative mechanism.

5. SUMMARY

In this review we investigated on the multiband superconductivity. We consider the physical properties of superconductor MgB_2 and use our two-band model to explain the two coupled superconductor's gaps of MgB_2.

The discovery of a new types of high-temperature superconductivity in MgB_2 and FeAS system generates expectations of the appearance of novel superconductors with higher T_c and room temperature superconductors.[54,55]

References and Notes

1. H. Nagao, S. P. Kruchinin, A. M. Yaremko, and K. Yamaguchi, Multiband superconductivity. *Int. J. Mod. Phys. B* 16, 3419 **(2002)**.
2. S. P. Kruchinin and H. Nagao, Two-gap superconductivity in MgB. *Phys. Particles Nuclei* 36, 127 **(2005)**.
3. S. P. Kruchinin and A. M. Yaremko, Many zone effect in cuprate superconductors. *Supercond. Sci. Technol.* 11, 4 **(1998)**.
4. H. Nagao, H. Kawabe, S. P. Kruchinin, D. Manske, and K. Yamaguchi, Theoretical studies on many band effects superconductivity by using renormalization group approach. *Mod. Phys. Lett. B* 17, 423 **(2003)**.
5. H. Nagao, H. Kawabe, S. P. Kruchinin, and K. Yamaguchi, Superconductivity in two-band model by renormalization group approach. *Int. J. Mod. Phys. B* 17, 3373 **(2003)**.
6. A. M. Yaremko, E. V. Mozdor, and S. P. Kruchinin, Coupled states of electron-phonon system, superconductivity and HTSC of crystals. *Int. J. Mod. Phys. B* 10, 2665 **(1996)**.
7. S. P. Kruchinin and H. Nagao, Multi-gap superconductivity in MgB_2, *Proc. NATO Advanced Research Workshop "Symmetry and Heterogeneity in High- Tc Superconductors,"* edited by A. Bianconi, Kluwer, Dorderecht **(2006)**, pp. 43–53.
8. H. Nagao, A. Yaremko, S. P. Kruchinin, and K. Yamaguchi, Many band effects in superconductivity, *Proc. NATO Advanced Research Workshop "New Trends in Superconductivity,"* edited by J. Annett and S. P. Kruchinin, Kluwer, Dordrecht **(2002)**, pp. 155–167.
9. S. P. Kruchinin, A. Zolotovsky, and H. T. Kim, Band structure of new ReFe AsO superconductors. *J. Modern Phys.* 4, 608 **(2013)**.
10. S. P. Kruchinin, Physics of high-T_c superconductors. *Review in Theoretical Physics* 2, 1 **(2014)**.
11. A. A. Abrikosov, L. P. Gorkov, and I. E. Dzyaloshinski, Methods of Quantum Field Theory in Statistical Physics, (Dover) **(1975)**.
12. L. A. Fetter and J. D. Walecka, Quantum Theory of Many-Particle Systems, McGraw-Hill **(1987)**.
13. J. G. Bednorz and K. A. Müller, Possible high-T_c superconductivity in the Ba–La–Cu–O system. *Z. Phys. B* 64, 189 **(1986)**.
14. P. W. Anderson, Theory of dirty superconductivity. *J. Phys. Chem. Solids* 11, 26 **(1959)**.
15. A. P. Kampf, Magnetic correlations in high temperature superconductivity. *Phys. Rep.* 249, 219 **(1994)**.
16. V. J. Emery, Theory of high-T_c superconductivity in oxides. *Phys. Rev. Lett.* 58, 2794 **(1987)**.
17. J. E. Hirsch, Attractive interaction and pairing in fermion systems with strong on-site repulsion. *Phys. Rev. Lett.* 25, 1317 **(1985)**.
18. F. C. Zhang and T. M. Rice, Effective Hamiltonian for the superconducting Cu oxides. *Phys. Rev. B* 37, 3759 **(1988)**.
19. E. Fradkin, Field Theories of Condensed Matter Systems, Addison Wesley **(1991)**.
20. N. Nagaosa and P. A. Lee, Normal-state properties of the uniform resonating-valence-bond state. *Phys. Rev. Lett.* 64, 2450 **(1990)**.
21. G. Baskaran, Z. Zou, and P. W. Anderson, The resonating valence bond state and high-T_c superconductivity—a mean field theory. *Solid State Commun.* 63, 973 **(1987)**.
22. H. Fukuyama and K. Yoshida, Critical temperature of superconductivity caused by strong correlation. *Jpn. J. Appl. Phys.* 26, 371 **(1987)**.
23. S. Yamamoto, K. Yamaguchi, and K. Nasu, *Ab initio* molecular-orbital study on electron correlation effects in CuO_6 clusters relating to high-T_c superconductivity. *Phys. Rev. B* 42, 266 **(1990)**.

24. H. Nagao, H. Nishino, Y. Shigeta, and K. Yamaguchi, Theoretical studies on anomalous phases of photodoped systems in two-band model. *J. Chem. Phys.* 113, 11237 **(2000)**.

25. H. Nagao, Y. Kitagawa, T. Kawakami, T. Yoshimoto, H. Saito, and K. Yamaguchi, Theoretical studies on field-induced superconductivity in molecular crystals. *Int. J. Quantum Chem.* 85, 608 **(2001)**.

26. M. Kimura, H. Kawabe, A. Nakajima, K. Nishikawa, and S. Aono, Possibility of superconducting and other phases in organic high polymers polyacene carbon skeletons. *Bull. Chem. Soc. Jpn.* 61, 4239 **(1988)**.

27. N. N. Bogoliubov and S. Tyablikov, Retarded and advanced Green functions in statistical physics. *Dokl. Acad. Sci. USSR* 126, 53; *Sov. Phys. Dokl.* 4, 589 **(1959)**.

28. P. Konsin and B. Sorkin, Electric field effects in high-T_c cuprates. *Phys. Rev. B* 58, 5795 **(1998)**.

29. H. Nagao, M. Nishino, Y. Shigeta, Y. Yoshioka, and K. Yamaguchi, Theoretical studies on superconducting and other phases: Triplet superconductivity, ferromagnetism, and ferromagnetic metal. *J. Chem. Phys.* 113, 721 **(2000)**.

30. H. Suhl, B. T. Matthias, and R. Walker, Bardeen-Cooper-Schrieffer theory of superconductivity in the case of overlapping bands. *Phys. Rev. Lett.* 3, 552 **(1959)**.

31. V. A. Moskalenko, Superconductivity metals with overlapping energetic bands. *Fiz. Metalloved* 8, 503 **(1959)**.

32. J. Kondo, Superconductivity in transition metals. *Prog. Theor. Phys.* 29, 1 **(1963)**.

33. E. Antipov and A. Abakumov, Structural design of superconductors based on complex copper oxides. *Phys. Usp.* 51, 180 **(2008)**.

34. K. A. Müller, The search for new high temperature superconductors. *Supercond. Sci. Technol.* 58, 1 **(2006)**.

35. J. Nagamatsu, N. Nakamura, T. Muranaka, Y. Zentani, and J. Akimitsu, Superconductivity at 39 K in magnezium deboride. *Nature* 410, 63 **(2001)**.

36. K. H. Bennemann and J. B. Ketterson, Superconductivity, Springer, Heidelberg **(2008)**, Vol. 1.

37. T. Ord, N. Kristoffel, and K. Rago, MgB_2 superconductivity properties in a two-gap model, *Mod. Phys. Lett. B* 17, 667 **(2003)**.

38. Y. Doi and S. Aono, Theory of line shape in nuclear magnetic resonance. *Prog. Theor. Phys.* 51, 1019 **(1974)**.

39. J. Kortus, I. I. Mazin, K. D. Belashenko, V. P. Antropov, and I. L. Boyer, Superconductivity of metallic boron in MgB_2. *Phys. Rev. Lett.* 86, 4656 **(2001)**.

40. J. P. C. Canfield, S. L. Bud'ko, and D. K. Finnemore, An overview of the basic physical properties of MgB_2. *Physica C* 385, 1 **(2003)**.

41. N. Kristoffel, T. Ord, and K. Rago, MgB_2 two-gap superconductivity with intra- and interband couplings. *Europhys. Lett.* 61, 109 **(2003)**.

42. G. Binnig, A. Baratoff, H. E. Hoenig, and J. G. Bednorz, Two-band superconductivity in Nb-doped $SrTiO_3$. *Phys. Rev. Lett.* 45, 1352 **(1980)**.

43. J. M. An and W. E. Picket, Superconductivity of MgB_2: Covalent bonds driven metallic. *Phys. Rev. Lett.* 86, 4366 **(2001)**.

44. P. Szabo, P. Samuely, T. Klein, J. Marcus, D. Fruchart, S. Miraglia, C. Marcenat, and A. Jansen, Evidence for two superconducting energy gaps in MgB_2 by point-contact spectroscopy. *Phys. Rev. Lett.* 87, 137005 **(2001)**.

45. W. L. McMillan, Transition temperature of strong-coupled superconductors. *Phys. Rev.* 167, 331 **(1968)**.

46. H. Nagao, M. Mitani, M. Nishino, Y. Shigeta, Y. Yoshioka, and K. Yamaguchi, Theoretical studies on anomalous phases in molecular systems with external field: Possibility of photo-induced superconductivity. *Int. J. Quantum Chem.* 75, 549 **(1999)**.

47. H. Nagao, M. Nishino, Y. Shigeta, Y. Yoshioka, and K. Yamaguchi, Theoretical studies on superconducting and other phases: Triplet superconductivity, ferromagnetism, and ferromagnetic metal. *J. Chem. Phys.* 113, 721 **(2000)**.

48. H. Nagao, M. Nishino, M. Mitani, Y. Yoshioka, and K. Yamaguchi, Possibilities of charge- and/or spin-mediated superconductors and photo-induced superconductors in the intermediate region of metal-insulator transitions. *Int. J. Quantum Chem.* 65, 947 **(1997)**.

49. N. N. Bogoliubov and D. V. Shirkov, Introduction to the Theory of Quantized Field, Interscience, New York **(1959)**.

50. M. Kimura, H. Kawabe, K. Nishikawa, and S. Aono, Possibility of superconducting and other phases in organic high polymers of polyacene carbon skeletons II: screened electron–electron interaction. *Bull. Chem. Soc. Jpn.* 61, 4245 **(1988)**.

51. M. Kimura, H. Kawabe, K. Nishikawa, and S. Aono, Superconducting and other phases in organic high polymers of polyacenic carbon skeletons I: The method of sum of divergent perturbation series. *J. Chem. Phys.* 85, 3090 **(1986)**.

52. M. Kimura, H. Kawabe, K. Nishikawa, and S. Aono, Superconducting and other phases in organic high polymers of polyacenic carbon skeletons II: The mean field method. *J. Chem. Phys.* 85, 3097 **(1985)**.

53. M. Kimura, H. Kawabe, A. Nakajima, K. Nishikawa, and S. Aono, Possibility of superconducting and other phases in organic high polymers of polyacene carbon skeletons II: Screened electron–electron interaction. *Bull. Chem. Soc. Jpn.* 61, 4239 **(1988)**.

54. R. Mankowsky, A. Subedi, M. Först, S. O. Mariager, M. Chollet, H. T. Lemke, J. S. Robinson, J. M. Glownia, M. P. Minitti, A. Frano, M. Fechner, N. A. Spaldin, T. Loew, B. Keimer, A. Georges, and A. Cavalleri, Nonlinear lattice dynamics as a basis for enhanced superconductivity in $YBa_2Cu_3O_{6.5}$. *Nature* 516, 71 **(2014)**.

55. S. Kaiser, et al., Optically induced coherent transport far above T_c in underdoped $YBa_2Cu_3O_{6+\delta}$. *Phys. Rev. B* 89, 184516 **(2014)**.